



Quantum interference effects in two double quantum dots-molecules embedded in an Aharonov–Bohm ring

M.L. Ladrón de Guevara^{a,*}, G.A. Lara^b, P.A. Orellana^a

^a Universidad Católica del Norte, Casilla 1280, Antofagasta, Chile

^b Universidad de Antofagasta, Casilla 170, Antofagasta, Chile

ARTICLE INFO

Article history:

Received 17 December 2009

Accepted 11 January 2010

Available online 15 January 2010

Keywords:

Electronic transport

Quantum dots

Quantum interference

ABSTRACT

We study equilibrium and non-equilibrium transport of non-interacting electrons through two quantum dot molecules embedded in an Aharonov–Bohm interferometer, and focus in several quantum interference effects occurring in both regimes. We obtain analytical expressions for the transmission and the density of states, and we calculate numerically the current at zero temperature. We show that the system exhibits Fano resonances, total suppression of transmission, and bound states in the continuum. In equilibrium we find a magnetic flux-dependent *effective level attraction* and lines of perfect transmission when the intramolecular coupling is weak. This feature has strong consequences in the non-equilibrium regime, where the I - V characteristics displays a region of negative differential conductance induced by the magnetic flux. The current suffers an abrupt rise for small bias voltages as consequence of an effective level attraction of the hybridized levels produced by the flux. The decrease of current is result of the destruction of this effect when the bias is increased.

© 2010 Elsevier B.V. All rights reserved.

1. Introduction

Electron transport in systems of multiple quantum dots, and in particular in coupled double quantum dots (DQD), has been a subject of intensive research in recent years. The coupled DQD was initially studied in its similitude with a real molecule [1], but the interest on this system has turned to several other directions, as its possible use in spintronics [3] and quantum computing [2].

One of the key features of transport in quantum dots is the high degree of phase coherence of electrons, one of the basic quantum phenomena. Quantum coherence manifests in the presence of different electronic pathways, and this has motivated the study of quantum dot structures embedded in interferometers. Systems as a coupled DQD embedded in a ring [4–7], or ‘quantum dot molecule’, have received much attention recently for the variety of quantum interference effects they show. Experiments have allowed to observe in this structure Aharonov–Bohm (AB) oscillations of the conductance and Fano resonances [4,8,9], and theoretical works have predicted other quantum coherence consequences as Dicke effect [7] and bound states in the continuum [5]. The interplay of electronic interactions and quantum interference in the DQD embedded in a ring is explored in Refs. [10–14], showing no conventional behaviors in Kondo and Coulomb blockade regimes. Spin dependent transport

in the same system with ferromagnetic leads is considered in Refs. [15,16] and in the presence of Rashba spin–orbit interaction in Ref. [17].

From the application point of view, an interesting feature exhibited quantum dots is the negative differential conductance (NDC) [18]. NDC has been studied in single as well as in double quantum dot systems, and it has applications in amplifiers and oscillators in the microwave, mm-wave and Terahertz frequency ranges [19]. In multilevels quantum dots NDC can occur when states have different couplings to the leads [20–23]. In a serial double quantum dot, negative differential conductance can be produced when the bias breaks the transmission channel extended along the system [24]. Other theoretical works on generation of NDC in double quantum dot molecules connected in series are Refs. [25–29]. In a DQD embedded in an Aharonov–ring, magnetic-flux-induced NDC was found in the strong interdot repulsion regime [12]. A similar result was found by Mourokh and Smirnov in a double molecule with three terminals [30]. Recently, it was reported NDC induced by the electronic correlation in a side-coupled DQD [31].

Our work aims to study a system of two double quantum dot molecules in an Aharonov–Bohm interferometer. This system exhibits a phenomenology different from the DQD molecule in an AB ring, and it presents novel results in the situation out of equilibrium. This configuration resembles in some aspects to two uncoupled quantum dots in an AB interferometer [32] and it captures some of its physics, but a richer phenomenology arises from the fact that we are dealing with double quantum dots

* Corresponding author.

E-mail address: mlladron@ucn.cl (M.L. Ladrón de Guevara).

rather than single quantum dots. We model the system by a non-interacting Hamiltonian, which allows to describe most of the relevant phenomena associated to quantum interference, as mentioned above. We obtain analytical expressions for the transmission and the density of states, and we calculate numerically the current at zero temperature. We show that the transmission both in and out of equilibrium exhibits Fano resonances, total reflection, and suppressed peaks as a manifestation of bound states in the continuum (BICs). The BICs are resonances of vanishing linewidth, which can occur when resonances belonging to different channels interfere [33]. These have been demonstrated experimentally in semiconductor heterostructures grown by molecular beam epitaxy [34]. The occurrence of these states in quantum dots was discussed by us in a DQD and a triple QD embedded an interferometer [5,7,35]. There have been an increasing interest on BICs in different contexts [36–38].

Other aspect we addressed to is the presence of a flux-dependent *effective level attraction* and lines of perfect transmission [39,32] when the intramolecular coupling is weak. These features manifest in equilibrium and are destroyed progressively as the bias voltage is increased. In the non-equilibrium regime, we identify two kinds of NDC regions in the I - V characteristics, occurring at different scales and of different origin. One is generated by the usual mechanism of the NDC in a double quantum dot systems [24]. The current will increase or decrease with voltage, depending on whether the voltage makes the levels of the different quantum dots become aligned or not aligned. The other region occurs at smaller voltages and is induced by the magnetic flux. We explain the latter effect in terms of the destruction of the flux-induced level attraction by the bias.

2. Model

The system under consideration is shown in Fig. 1. Two equal double quantum dot molecules are embedded in an Aharonov–Bohm ring, which is attached to large contacts through one-dimensional leads. Equilibrium transport in a similar configuration with additional connections between dots was studied by Li et al. [40]. The left and right contacts are in thermodynamic equilibrium with thermodynamical potentials μ_L and μ_R , respectively. We consider only one level relevant in each of the quantum dots. The system is modeled by a non-interacting Anderson Hamiltonian, which can be written as $H = H_M + H_0 + H_I$, where H_M describes the dynamics of the isolate molecules,

$$H_M = \sum_{\alpha=+,-} \sum_{i=A,B} \varepsilon_i d_{i\alpha}^\dagger d_{i\alpha} + \sum_{\alpha=+,-} (t_\alpha d_{A,\alpha}^\dagger d_{B,\alpha} + t_\alpha^* d_{B,\alpha}^\dagger d_{A,\alpha}), \quad (1)$$

where $\varepsilon_{A(B)}$ is the level energy of the left (right) quantum dot in the molecule α ($\alpha = +, -$); $d_{i,\alpha}$ ($d_{i,\alpha}^\dagger$) annihilates (creates) an electron in dot i in the molecule α , and t_α is the intramolecular

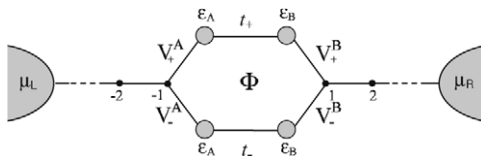


Fig. 1. Two double quantum dot molecules embedded in parallel in an Aharonov–Bohm interferometer.

tunneling hopping. H_0 is the Hamiltonian for the electrons in the leads

$$H_0 = \frac{V}{2} \sum_{i=-\infty}^{-1} c_i^\dagger c_i + v \sum_{i=-\infty}^{-1} (c_i^\dagger c_{i-1} + c_{i-1}^\dagger c_i) - \frac{V}{2} \sum_{i=1}^{\infty} c_i^\dagger c_i + v \sum_{i=1}^{\infty} (c_i^\dagger c_{i+1} + c_{i+1}^\dagger c_i), \quad (2)$$

where c_i (c_i^\dagger) is the annihilation (creation) operator of an electron in the site i -th of the leads, and v the hopping between sites in the leads. The term H_I accounts for the tunneling between molecules and leads,

$$H_I = - \sum_{\alpha=+,-} (V_\alpha^A d_{A\alpha}^\dagger c_{-1} + V_\alpha^{A*} c_{-1}^\dagger d_{A\alpha}) - \sum_{\alpha=+,-} (V_\alpha^B d_{B\alpha}^\dagger c_1 + V_\alpha^{B*} c_1^\dagger d_{B\alpha}) \quad (3)$$

with $V_\alpha^{A(B)}$, the tunneling coupling connecting the left (right) dot of the α -th molecule with the left (right) lead. We restrict to the case in which there is not magnetic field acting directly on the electrons, so that the situation will be identical for the two values of spin.

In the presence of a magnetic flux threading the ring, and using gauge invariance, we add the Aharonov–Bohm phase $\phi = 2\pi\Phi/\Phi_0$ around the ring by the replacement $V_+^A = t_A e^{-i\phi/6}$, $t_+ = t_c e^{-i\phi/6}$, $V_+^B = t_B e^{-i\phi/6}$, $V_-^A = t_A e^{i\phi/6}$, $t_- = t_c e^{i\phi/6}$, $V_-^B = t_B e^{i\phi/6}$, with $\Phi_0 = h/e$ the flux quantum. We look for the steady states $|\psi_k\rangle$ of the whole Hamiltonian H . The Hamiltonian describing the leads, H_0 , corresponds to a free-particle Hamiltonian on a lattice, the eigenfunctions being Bloch functions $|k_\beta\rangle = \sum_j e^{ik_\beta j} |j\rangle$, $\beta = L, R$, where $|k_\beta\rangle$ is the momentum eigenstate and $|j\rangle$ a Wannier state localized at the j -th site. The corresponding dispersion relations are $\varepsilon = V/2 - 2vcosk_L$, for the electrons originated in the left contact, and $\varepsilon = -V/2 - 2vcosk_R$ for those originated in the right contact. The eigenstates of the entire Hamiltonian can be written as

$$|\psi_k\rangle = \sum_{j=-\infty}^{-1} a_j^k |j\rangle + \sum_{\alpha=+,-} \sum_{i=A,B} b_{i,\alpha}^k |i, \alpha\rangle + \sum_{j=1}^{\infty} a_j^k |j\rangle \quad (4)$$

We assume electrons as described by a plane wave incident from the far left (right) with unit amplitude, reflection amplitude r (r'), and transmission amplitude t (t'), and solve the Schrödinger equation $H|\psi_k\rangle = E_k|\psi_k\rangle$ for a_j^k and $b_{i,\alpha}^k$. We are interested in the transmission and the current through the system for an applied voltage V/e between source and drain such that the site energy is $V/2$ for the left lead and $-V/2$ for the right lead. We center in the symmetrical configuration, that is, equal left and right dot-lead couplings, $t_A = t_B$. Additionally, we assume that the voltage drop occurs only between the dot A and the dot B, so that the energies of the quantum dots are equal to the site energies of the adjacent leads, $\varepsilon_A = V/2$ and $\varepsilon_B = -V/2$. At zero temperature, the current in the leads is given by

$$I(V) = \frac{2e}{h} \int_{-V/2}^{V/2} T(\varepsilon) d\varepsilon, \quad (5)$$

where $T(\varepsilon)$ is the transmission. We have assumed that the Fermi level in equilibrium is equal to 0.

3. Results

The transmission probability can be written in the form

$$T(\varepsilon) = \frac{4t_c^2 \Gamma^2(\Delta\varepsilon)^4 \cos^2 \phi/2}{A} \quad (6)$$

$A = [(\Delta\varepsilon)^4 + \Gamma^2(\varepsilon - q)^2][(\Delta\varepsilon)^4 + \Gamma^2(\varepsilon + q)^2]$, where $(\Delta\varepsilon)^2 = \varepsilon^2 - p^2$, with $p^2 = (V/2)^2 + t_c^2$ and $q^2 = (V/2)^2 + t_c^2 \cos^2(\phi/2)$, where $\Gamma = 4\pi t_A^2 \rho(0)$ is the characteristic line half-width, with $\rho(0)$ the density of states in the leads at the Fermi level.

It follows from the expression (6) that the transmission has a period $\Delta\phi = 2\pi$ ($\Delta\Phi = \Phi_0$) and that T identically vanishes when ϕ is an odd multiple of π ($\Phi = n\Phi_0/2$, n odd). This fully destructive interference effect for this value of ϕ is expected, since in the absence of magnetic flux the upper and lower paths are equivalent, then the flux introduces in the wave function a phase $-\pi/2$ along one arm and $\pi/2$ along the other. On the other hand, in the considered symmetry the transmission in general presents two Fano resonances superposed to two Lorentzians. When ϕ is an even multiple of π ($\Phi = n\Phi_0$, n integer), $T = 4t_c^2 \Gamma^2 / [(p^2 - \varepsilon^2)^2 + 2\Gamma^2(p^2 + \varepsilon^2) + \Gamma^4]$, that is, the Fano resonances disappear from the transmission, indicating the presence of two bound states in the continuum [5,7]. The BICs in this configuration are formed by the hybridization through the leads of the upper and lower molecular states.

3.1. Equilibrium transport

The equilibrium transmission is obtained from Eq. (6) by making $V = 0$. According to the intramolecular coupling we can distinguish two regimes, where transmission displays essentially different behaviors: $t_c \leq \Gamma/\sqrt{2}$ and $t_c > \Gamma/\sqrt{2}$. We will show that for weak intramolecular couplings the magnetic flux induces an effective attraction of the molecular levels analogous to that discussed in Ref. [39] in a quantum ring with two elastic scatterers. In Fig. 2 we have plotted $T(\varepsilon)$ for $t_c = 0.25\Gamma$, that is, an intramolecular coupling weak as compared to the coupling of the molecules to the contacts. In Fig. 2(a) (dash line) $\Phi = 0$ and t_c is small enough, that a single and flat peak is observed, with features very similar to those of a molecule in series with small intramolecular coupling. However, as commented above, two bound states in the continuum are occurring. This means that two of the molecular states are localized and do not participate of transmission [41]. These states become delocalized whenever the symmetry of the system is broken, as occurs when the magnetic flux is turned on. This is the case of Fig. 2(a) (solid line) and the rest of Fig. 2, where the two BICs are replaced by two Fano resonances. The Fano peaks reach $T = 1$. In Figs. 2(a)–(d) (solid line) it is evident a level attraction as the flux increases from 0 to

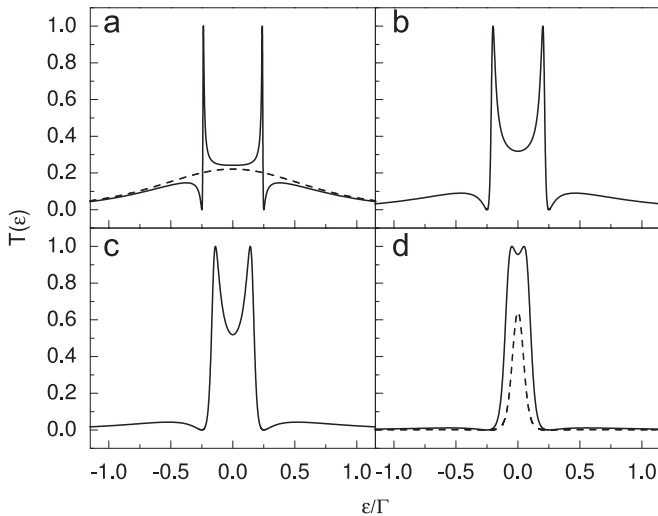


Fig. 2. Transmission versus energy for $t_c = 0.25\Gamma$ and (a) $\Phi = 0$ (dash line) and $\Phi = 0.1\Phi_0$ (solid line), (b) $\Phi = 0.2\Phi_0$, (c) $\Phi = 0.3\Phi_0$, (d) $\Phi = 0.4\Phi_0$ (solid line) and $\Phi = 0.46\Phi_0$ (dash line).

$\Phi_0/2$. The Fano peaks get progressively closer to each other until overlapping completely at a value close but lesser than $\Phi_0/2$. Then the transmission decays (dash line in Fig. 2(d)), until vanishing when $\Phi = \Phi_0/2$. The ‘level attraction’ induced by the magnetic flux is explained by the presence of resonances near the energies of the electronic states of the ring, the latter depending periodically on the magnetic flux. The sharpness of the resonances when the intramolecular couplings are weak occur by the multiple reflections of the electron in the ring, where the electron is transmitted only if it has an energy close to one of the eigenstates [39].

Let us examine now the positions of the resonances as a function of the magnetic flux. It follows from Eq. (6) that perfect transmission takes place at energies obeying the following equation:

$$\varepsilon^4 - \varepsilon^2(2t_c^2 - \Gamma^2) + t_c^2[t_c^2 - \Gamma^2 \cos^2(\phi/2)] = 0, \quad (7)$$

with the solutions $\varepsilon_1^\pm = \pm [A+B]^{1/2}$, $\varepsilon_2^\pm = \pm [A-B]^{1/2}$, with $A = t_c^2 - \Gamma^2/2$ and $B = (\Gamma/2)[\Gamma^2 - 4t_c^2 \sin^2(\phi/2)]^{1/2}$. Fig. 3(a) shows the positions of the $T = 1$ peaks for different values of $t_c \leq \Gamma/\sqrt{2}$. These correspond to ε_1^+ and ε_1^- , the only real solutions of Eq. (7). We have to note that the solutions for $\Phi = 0$ displayed in the plot are not physical, in accordance to Fig. 2(a) (dash line). In the three cases the peaks positions shift progressively to the center of the band as Φ increases. The peaks meet at $\varepsilon = 0$ at $\Phi = \arccos(t_c/\Gamma)\Phi_0/\pi$. The situation changes when $t_c > \Gamma/\sqrt{2}$, where ε_1^+ and ε_1^- stop meeting at $\varepsilon = 0$ and the solutions ε_2^+ and ε_2^- become real in a range of Φ , as shown in Fig. 3(b) (dash lines). As observed, the solutions ε_1^- (ε_1^+) and ε_2^- (ε_2^+) meet, but there is not level attraction into the center of the band as the flux increases.

Let us examine how the just described features affect the shape of the Aharonov–Bohm oscillations of the conductance $G = (2e^2/h)T(\mu = 0)$. G is given as a function of the flux by

$$G = \frac{2e^2}{h} \frac{4\cos^2(\pi\Phi/\Phi_0)(t_c/\Gamma)^2}{[\cos^2(\pi\Phi/\Phi_0) + (t_c/\Gamma)^2]}. \quad (8)$$

We distinguish in Eq. (8) two different behaviors. When $t_c \leq \Gamma$ there is always a value of Φ for which $T(0) = 1$, while when $t_c > \Gamma$ this never occurs. This features are understood from the $T = 1$ peaks positions shown in Figs. 3(a) and (b). Fig. 4, which shows the conductance versus the magnetic flux for different values of the t_c . For $t_c = 0.05\Gamma$ and $t_c = 0.25\Gamma$, the conductance is symmetric around $\Phi_0/2$, reaching the maximum $G = 2e^2/h$ at $\Phi = \arccos(t_c/\Gamma)\Phi_0/\pi$. These features are repeated for all t_c in the

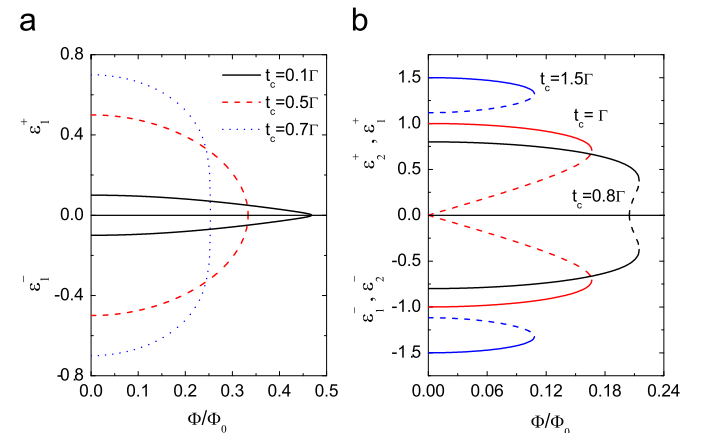


Fig. 3. (a) Positions of the $T = 1$ peaks for different values of $t_c \leq \Gamma/\sqrt{2}$: $t_c = 0.1\Gamma$ (solid line), $t_c = 0.5\Gamma$ (dash line) and $t_c = 0.7\Gamma$ (dotted line) and (b) positions of the $T = 1$ peaks for $t_c > \Gamma/\sqrt{2}$. The solid lines correspond to ε_1^+ and ε_1^- , and the dash lines to ε_2^+ and ε_2^- .

interval $t_c \leq \Gamma$, and the smaller the value of t_c the sharper the maximum. This means that the fall of the transmission to zero described in Fig. 2(d) is more abrupt for smaller intramolecular couplings. Smoother oscillations are observed for $t_c > \Gamma$, where G never reaches $2e^2/h$.

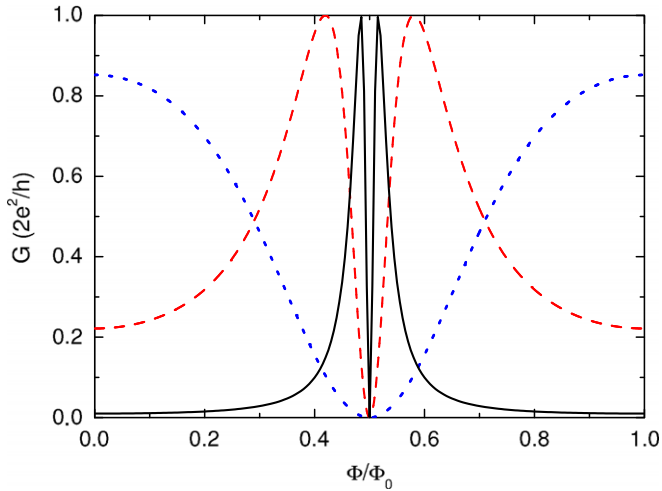


Fig. 4. (Color online) Conductance versus magnetic flux for $t_c = 0.05\Gamma$ (solid line), $t_c = 0.25\Gamma$ (dash line) and $t_c = 1.5\Gamma$ (dotted line).

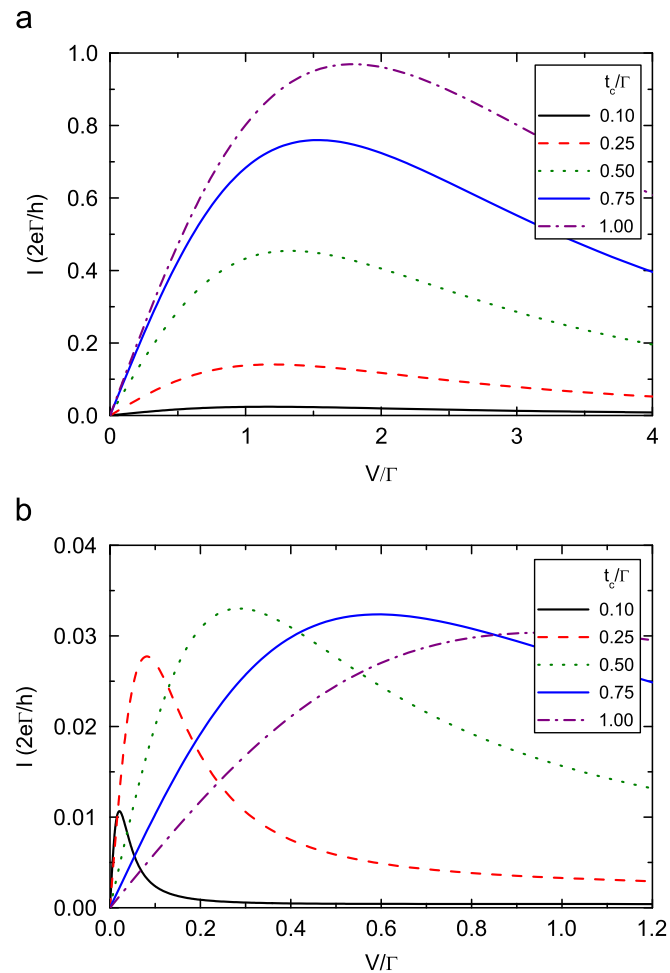


Fig. 5. (Color online) I - V characteristics for (a) $\Phi = 0$ and (b) $\Phi = 0.46\Phi_0$, and $t_c = 0.1\Gamma$ (solid line), $t_c = 0.25\Gamma$ (dash line), $t_c = 0.5\Gamma$ (dotted line), $t_c = 0.75\Gamma$ (dash-dotted line), $t_c = \Gamma$ (short dash line).

3.2. Non-equilibrium transport

Let us now consider a voltage V applied between contacts and let us study the current in the leads. Fig. 5(a) shows the current-voltage characteristics for $\Phi = 0$ and different values of intramolecular couplings. In all cases the current-voltage characteristics displays a peak, with the corresponding region of NDC. This behavior is typical of the serial QD [24]. The current increases when the bias allows a transmission channel exists along the left and right sides of the system. If the bias continues to increase, the channel is destroyed resulting in the drop of current. The destruction of this channel occurs because the molecular state allowing transmission is broken, and the electronic state gets localized in one of the quantum dots.

The existence of a magnetic flux produces changes in the I - V characteristics which become important when $t_c < \Gamma/\sqrt{2}$ and Φ is within an interval close to $\Phi_0/2$, as illustrated in Fig. 5(b), where $\Phi = 0.46\Phi_0$. We observe sharper current peaks at lower voltages as compared to the case $\Phi = 0$. The abrupt increase of the current at low voltages for small t_c is a consequence of the level attraction discussed for zero bias. To visualize this we have plotted in Fig. 6(a) the I - V characteristics for a fixed t_c and Φ , and in Fig. 6(b) the transmission spectra associated to the bias voltages indicated in the current curve. As observed, for small bias (cases 1–3) the transmission keeps large in all the transport region ($-V/2 < \varepsilon < V/2$), due to the existence of two overlapped resonances close to each other. Larger bias voltages make the heights of the resonances fall, so that the transmission in all the window of transport becomes smaller, occurring the observed decrease in the current. A further insight of this is obtained through the density of states of the left and right quantum dots.

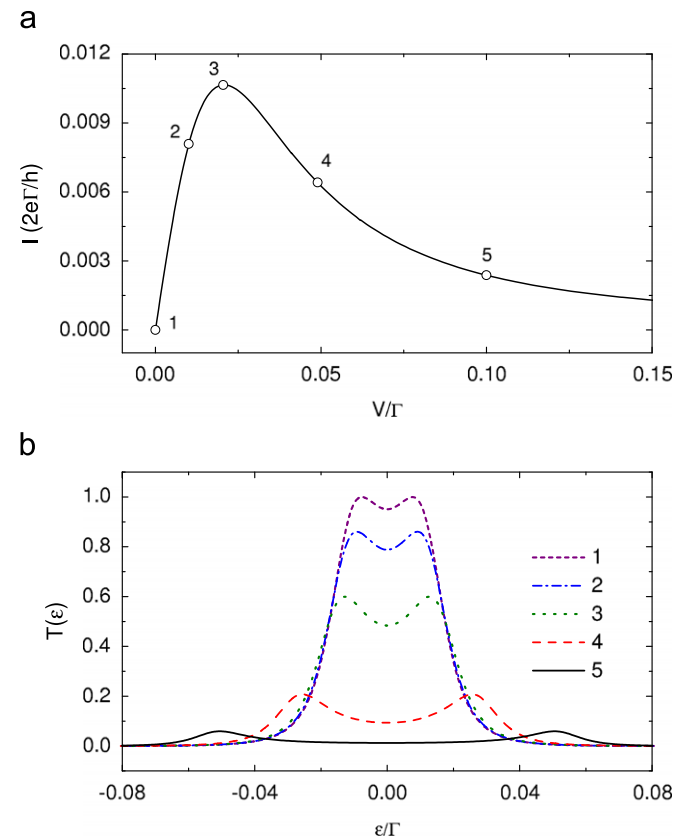


Fig. 6. (Color online) (a) I - V characteristics for $t_c = 0.1\Gamma$ and $\Phi = 0.46\Phi_0$. (b) Transmission spectrum for the same parameters and the values of voltages corresponding to the indicated points in (a).

The DOS for electrons coming from the left

$$\rho_A = s_L \frac{(\varepsilon_p c_R - t_c^2 c_\theta^2)^2 + \varepsilon_p^2 s_R^2 + t_c^4 s_\theta^2 c_\theta^2}{\pi \Delta^2 D^2}, \quad (9)$$

$$\rho_B = s_L t_c^2 \frac{(c_R - \varepsilon_n c_\theta^2)^2 + s_R^2 + \varepsilon_n^2 s_\theta^2 c_\theta^2}{\pi \Delta^2 D^2}, \quad (10)$$

where $D^2 = (c_L c_R - s_L s_R - t_c^2 c_\theta^2)^2 + (s_L c_R + s_R c_L)^2$, $s_\theta = \sin(\theta/2)$, $c_\theta = \cos(\theta/2)$, $\Delta^2 = \varepsilon_p \varepsilon_n - t_c^2$ and

$$\varepsilon_n = \varepsilon - V_0/2, \quad \varepsilon_p = \varepsilon + V_0/2,$$

$$c_L = \varepsilon_p - r \Delta^2 \varepsilon_n, \quad c_R = \varepsilon_n - r \Delta^2 \varepsilon_p,$$

$$s_L = \Delta^2 \sqrt{1 - r^2 \varepsilon_n^2}, \quad s_R = \Delta^2 \sqrt{1 - r^2 \varepsilon_p^2},$$

where $r = \Gamma/2t$. ρ_A (ρ_B) corresponds to the sum of the densities of states in the dots A (B) of both arms. Fig. 7 shows the left and right quantum dots DOS for the same parameters of Fig. 6. In equilibrium ($V = 0$) a molecular state is formed. For the cases 2 and 3 the coherence is still preserved but for higher voltages (cases 4–5) the physical picture changes. In these cases, the coherence between dots is lost, the electron is localized at the left quantum dots and the molecular bridge is broken. It is important to remark that the just discussed features does not exist if the magnetic flux is absent, so that in this case we can talk of a magnetic flux-induced NDC. Flux-induced NDC is discussed in a parallel DQD molecule embedded in an Aharonov–Bohm ring [12] and in a molecule in a three terminals configuration [30], in both cases NDC occurs in the strong interdot repulsion limit.

It is valid to ask how sensitive are the above results to the choice of the voltage drop across the ring. We have chosen a potential drop equal to V between the left and right dots, each of them being at the same voltage than the adjacent lead [24]. This assumption is reasonable in quantum dots, since the energies of the individual dots can be tuned to the desired value through gate voltages. We have explored other voltage drops, finding that flux-induced NDC exists whenever the left and right quantum dots are at different potentials, no matter how small such difference. The effect is strengthened when $\mu_L = V/2 = -\mu_R$ and $\varepsilon_A = V/4 = -\varepsilon_B$, and it vanishes when $\varepsilon_A = \varepsilon_B$.

We expect that the above picture remains valid even if the electron–electron interaction is considered. In fact, in embedded QD arrays, the main effect of the electron–electron interaction is to shift and to split the resonances [42]. This occurs because the

on-site Coulomb repulsion energy U introduces a renormalization of the site energies. In analogy with QD arrays in series, we expect that depending on the relation between the interdot coupling and the on-site Coulomb interaction different regimes arise. For $t_c/U \ll 1$, the resonances and antiresonances would split into two distinct minibands separated by the on-site Coulomb energy, while for $t_c/U \gg 1$, the resonances and antiresonances would occur in pairs. This behavior should not break the negative differential conductance. On the other hand, in the limit of low temperatures and strong electronic correlations, as in the Kondo regime, both the energy levels and the interdot and dot-leads couplings are renormalized to values which depend non-linearly on parameters such as gate voltage and occupation number. Even though, we think it is possible, by modifying the control parameters, to attain the main effects described in this article. We would expect that the NDC were strengthened and nonlinear effects occurred, as in quantum dots in series and side-coupled in the Kondo regime [24,25,31,43]. A work in this direction is under progress.

4. Summary

In this work we have studied equilibrium and non-equilibrium transport through two quantum dot molecules embedded in an Aharonov–Bohm interferometer. We obtained analytical expressions for the transmission and the density of states, and we calculate numerically the current at zero temperature. In both, equilibrium and non-equilibrium, the transmission displays Fano resonances, total reflection and bound states in the continuum. In equilibrium, it shows a magnetic flux-dependent effective level attraction and lines of perfect transmission when the intramolecular coupling is weak.

In the non-equilibrium regime, we identify two kinds of NDC regions in the I – V characteristics, occurring at different scales and of different origin. A first current peak exists at voltages of the order of the characteristic linewidth Γ , and it is independent of the magnetic flux. The drop of current with the increase of bias has analogous explanation to the NDC region in a serial DQD. A second peak in the I – V characteristics takes place at voltages of the order of $\Gamma/100$, it occurs for small t_c and it is strongly dependent on the magnetic flux. In fact, it does not exist if the flux is absent. The current suffers an abrupt rise for small bias voltages, as consequence of an effective level attraction of the hybridized levels produced by the flux. The decrease of current is result of the destruction of this effect when the bias is increased.

Acknowledgments

The authors acknowledge financial support from FONDECYT, under Grant 1080660. M.L.L. de G. thanks financial support from Milenio ICM P06-067-F, and P.A.O. and G.A.L. from CONICYT/Programa Bicentenario de Ciencia y Tecnología (CENAVA, Grant ACT27).

References

- [1] W.G. van der Wiel, S. De Franceschi, J.M. Elzerman, T. Fujisawa, S. Tarucha, L.P. Kouwenhoven, *Rev. Modern Phys.* 75 (2003) 1.
- [2] D.P. DiVincenzo, *Science* 309 (2005) 2173; J.M. Taylor, J.R. Petta, A.C. Johnson, A. Yacoby, C.M. Marcus, M.D. Lukin, *Phys. Rev. B* 76 (2007) 035315.
- [3] S. Das Sarma, J. Fabian, X.D. Hu, I. Zutic, *Superlattices Microstruct.* 27 (2000) 289.
- [4] A.W. Holleitner, C.R. Decker, H. Qin, K. Eberl, R.H. Blick, *Phys. Rev. Lett.* 87 (2001) 256802.
- [5] M.L. Ladrón de Guevara, F. Claro, P.A. Orellana, *Phys. Rev. B* 67 (2003) 195335.
- [6] K. Kang, S.-Y. Cho, *J. Phys. Condens. Matter* 16 (2004) 117.

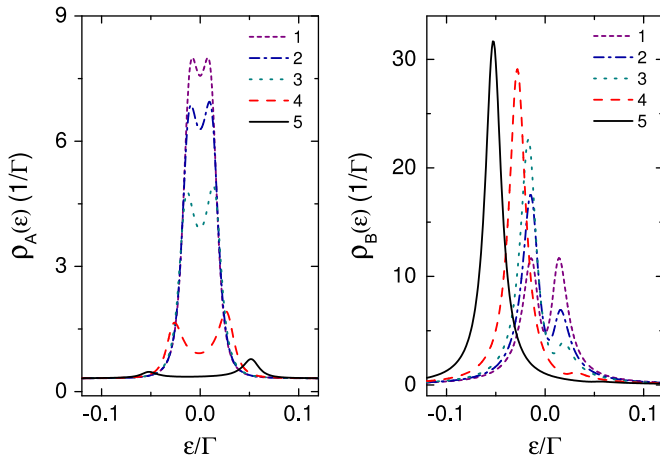


Fig. 7. (Color online) Densities of states of the electrons coming from the left at the quantum dots A and B , for $t_c = 0.1\Gamma$ and $\Phi = 0.46\Phi_0$, for the same voltages of Fig. 6(b).

- [7] P.A. Orellana, M.L. Ladrón de Guevara, F. Claro, *Phys. Rev. B* 70 (2004) 233315.
- [8] M. Sigrist, T. Ihn, K. Ensslin, D. Loss, M. Reinwald, W. Wegscheider, *Phys. Rev. Lett.* 96 (2006) 036804.
- [9] T. Ihn, M. Sigrist, K. Ensslin, W. Wegscheider, M. Reinwald, *New J. Phys.* 9 (2007) 111.
- [10] G.H. Ding, C.K. Kim, K. Nahm, *Phys. Rev. B* 71 (2005) 205313.
- [11] D. Sztienkiel, R. Swirkowicz, *J. Phys. Condens. Matter* 19 (2007) 176202.
- [12] B. Dong, X.L. Lei, N.J.M. Horing, *Phys. Rev. B* 77 (2008) 085309.
- [13] A. Ramsak, J. Mravlje, R. Zitko, J. Bonca, *Phys. Rev. B* 74 (2006) 241305 (R).
- [14] D. Sztienkiel, R. Swirkowicz, *J. Phys. Condens. Matter* 19 (2007) 386224.
- [15] P. Trocha, J. Barnas, *Phys. Rev. B* 76 (2007) 165432.
- [16] P. Trocha, I. Weymann, J. Barnas, *Phys. Rev. B* 80 (2009) 165333.
- [17] F. Chi, J.-L. Liu, L.-L. Sun, *J. Appl. Phys.* 101 (2007) 093704.
- [18] J. Weis, R.J. Haug, K.v. Klitzing, K. Ploog, *Phys. Rev. Lett.* 71 (1993) 4019.
- [19] T.C.L.G. Sollner, P.E. Tannenwald, D.D. Peck, W.D. Goodhue, *Appl. Phys. Lett.* 45 (1984) 1319.
- [20] D. Weinmann, W. Häusler, B. Kramer, *Phys. Rev. Lett.* 74 (1995) 984.
- [21] M. Ciorga, M. Pioro-Ladriere, P. Zawadzki, P. Hawrylak, A.S. Sachrajda, *Appl. Phys. Lett.* 80 (2002) 2177.
- [22] A. Thielmann, M.H. Hettler, J. König, G. Schön, *Phys. Rev. B* 71 (2005) 045341.
- [23] M.C. Rogge, F. Cavaliere, M. Sasseti, R.J. Haug, B. Kramer, *New J. Phys.* 8 (2006) 298.
- [24] R. Aguado, D.C. Langreth, *Phys. Rev. Lett.* 85 (2000) 1946.
- [25] P.A. Orellana, G.A. Lara, E.V. Anda, *Phys. Rev. B* 65 (2002) 155317.
- [26] J. Fransson, O. Eriksson, *J. Phys. Condens. Matter* 16 (2004) L85; J. Fransson, O. Eriksson, *Phys. Rev. B* 70 (2004) 085301.
- [27] B. Wunsch, M. Braun, J. König, D. Pfannkuche, *Phys. Rev. B* 72 (2005) 205319.
- [28] V.H. Nguyen, V.L. Nguyen, P. Dollfus, *Appl. Phys. Lett.* 87 (2005) 123107.
- [29] J.N. Pedersen, B. Lassen, A. Wacker, M.H. Hettler, *Phys. Rev. B* 75 (2007) 235314.
- [30] L.G. Mourokh, A.Y. Smirnov, *Phys. Rev. B* 72 (2005) 033310.
- [31] G.A. Lara, P.A. Orellana, E.V. Anda, *Phys. Rev. B* 78 (2008) 045323.
- [32] B. Kubala, J. König, *Phys. Rev. B* 65 (2002) 245301.
- [33] H. Friedrich, D. Wintgen, *Phys. Rev. A* 31 (1985) 3964; H. Friedrich, D. Wintgen, *Phys. Rev. A* 32 (1985) 3231.
- [34] F. Capasso, C. Sirtori, J. Faist, D.L. Sivico, S.-N.G. Chu, A.Y. Cho, *Nature* 358 (1992) 565.
- [35] M.L. Ladrón de Guevara, P.A. Orellana, *Phys. Rev. B* 73 (2006) 205303.
- [36] H. Nakamura, N. Hatano, S. Garmon, T. Petroky, *Phys. Rev. Lett.* 99 (2007) 210404.
- [37] N. Moiseyev, *Phys. Rev. Lett.* 102 (2009) 167404.
- [38] D.C. Marinica, A.G. Borisov, S.V. Shabanov, *Phys. Rev. Lett.* 100 (2008) 183902.
- [39] B. Büttiker, Y. Imry, M.Ya. Azbel, *Phys. Rev. A* 30 (1984) 1982.
- [40] Y.-X. Li, H.-Y. Choi, H.-W. Lee, *Phys. Lett. A* 372 (2008) 2073.
- [41] M.L. Ladrón de Guevara, G.A. Lara, P.A. Orellana, *Microelectron. J.* 39 (2008) 1304.
- [42] J.C. Chen, A.M. Chang, M.R. Melloch, *Phys. Rev. Lett.* 92 (2004) 176801.
- [43] G.A. Lara, P.A. Orellana, E.V. Anda, *Solid State Comm.* 125 (2003) 165.